Süleyman Demirel Üniversitesi
Fen Bilimleri Enstitüsü Dergisi
Cilt 26, Sayı 2, 275-284, 2022

Süleyman Demirel University
Journal of Natural and Applied Sciences
Volume 26, Issue 2, 275-284, 2022

DOI: 10.19113/sdufenbed.1056646

Relationship of photocatalysis with flavonoids in silver nanowire synthesis with herbal extract (*Lavandula officinalis* L.)

Havva KAYA[*1], **Semra KILIÇ**[2]

[1,]Suleyman Demirel Univesity, Department of Bioengineering, 32260, Isparta, Turkiye
[2] Suleyman Demirel Univesity, Faculty of Science and Art, Department of Biology, 32260, Isparta, Turkiye

(Alınış / Received: 12.01.2022, Kabul / Accepted: 02.03.2022, Online Yayınlanma / Published Online: 20.08.2020)

Keywords
Light radiation,
Nanoparticles,
Nanowires,
Phyto-nano synthesis,
Green synthesis

Abstract: Nanoparticles with unique physiochemical properties can be produced using non-toxic precursors with phyto-nano synthesis. In this study, Nanowire (AgNW) was produced from silver nanoparticles (AgNP) reduced with *Lavandula officinalis* L. flower extract using the phyto-nano synthesis method. The length of the produced AgNW is 1-20 µm and its diameter is approximately 40-100 nm. Although the reduction of silver was quite fast in the light environment, it was found to be slow in the dark environment. However, the effect of darkness on AgNP stabilization and AgNW formation was quite important. In addition, it was revealed that the main physical factor that enables AgNW to elongate is the mechanics of the environment provided by the centrifuge. Optical and morphological characterization of nanoparticles was done with UV-visible spectrometry and SEM. The crystal structure of the particles was determined by XRD. Energy dispersion spectrums of nanoparticles were determined by EDS. Character and size analysis was performed by TEM. FTIR determination was performed on the extracts to guide the determination of the reduction factors in light and dark. The extracts were also determined by HPLC to give an idea about the role of flavonoid content in the Ag reduction due to light. Accordingly, it was found that aromatic ring compounds with alcoholic groups effectively reduce silver in the dark and promote AgNW formation.

Bitki ekstraktı (*Lavandula officinalis* L.) ile gümüş nanotel sentezinde fotokatalizin flavonoidler ile ilişkisi.

Anahtar Kelimeler
Işık radyasyonu,
Nano parçacıklar,
Nano teller,
Fito-nano sentez,
Yeşil sentez

Öz: Benzersiz fizikokimyasal özelliklere sahip nanopartiküller, toksik olmayan öncüler kullanılarak fito nano sentez ile üretilebilir. Bu çalışmada, *Lavandula officinalis* L. çiçek özütü ile indirgenmiş gümüş nanoparçacıklardan (AgNP) fito-nano sentez yöntemi kullanılarak Nanotel (AgNW) üretilmiştir. Üretilen AgNW'nin uzunluğu 1-20 µm ve çapı yaklaşık 40-100 nm olarak tesbit edilmiştir. Gümüşün indirgenmesi aydınlık ortamda oldukça hızlı olmasına rağmen karanlık ortamda yavaş olduğu görülmüştür. Bununla beraber karanlığın AgNP stabilizasyonu ve AgNW oluşumu üzerinde kayda değer etkisi olmuştur. Ayrıca AgNW'nin uzamasını sağlayan ana fiziksel faktörün santrifüjün sağladığı ortamın mekaniği olduğu bulunmuştur. Nanopartiküllerin optik ve morfolojik karakterizasyonu UV-Vis spektrometri ve SEM ile yapıldı. Partiküllerin kristal yapısı XRD ile belirlendi. Nanopartiküllerin enerji dağılım spektrumları EDS ile belirlendi. Karakter ve boyut analizi TEM ile yapıldı. Aydınlık ve karanlıktaki indirgeme faktörlerinin belirlenmesine rehberlik etmek için ekstraktlar üzerinde FTIR yapıldı. Ayrıca, ışık ile Ag indirgenmesindeki flavonoid içeriğinin rolü hakkında bir fikir vermesi için numunlere HPLC yapıldı. Buna göre, alkollü gruplara sahip aromatik halkalı bileşiklerinin karanlıkta gümüşü etkili bir şekilde indirgediği ve AgNW oluşumunu teşvik ettiği sonucuna varıldı.

*İlgili yazar: kaya_havva@yahoo.com.tr

1. Introduction

Metal nanomaterials have influenced many branches of science such as engineering, health, environmental improvement studies with their versatile properties [1]. Silver shows very high electrical and thermal conductivity. For this reason, nanosilver is used in many engineering fields. Silver nanoparticles (AgNP) smaller than 100 nm in diameter can easily pass through the cell membrane and show activity in metabolic pathways. In this way, AgNP stands out as antibacterial, antioxidant, anti-cancer, and antifungal [2]. It is also used directly or by hybridizing with other metals in the fields of electrical, energy, biomedical engineering [3]. In addition to AgNP, silver nanowires (AgNW) are also used in flexible, transparent, wearable electronics [4], various optics [5], biomedical applications [6], solar cells [7]. There are chemical, physical, and biological methods in the production of both nanomaterials. In AgNW synthesis, it is possible to use electrochemical and hydrothermal methods, usually together with the reduction of silver salts [8]. Although for mass production of AgNW, standard size and high efficiency provided methods are preferred. One of the main methods in which carbon nanotubes or nanoporous molds are used as templates is hard-template nanowire synthesis. The other method is the soft-template nanowire synthesis technique in a non-solid medium such as polyol solvent with micelles, surfactants, and other polymers [9]. That is the most common method used to meet the AgNW requirement of the industry. Unfortunately, these methods generate a large amount of solvent and a large amount of waste that cannot be recycled easily. Recently, the technique of using plant extracts in the reduction of metal nanoparticles (phyto-nano synthesis) has been drawing attention in terms of being so simple and ecological. And also the reduction takes place in one step.

Components of essential oils such as linalool, caryophyllene, lavandulyl acetate, α-terpineol, borneol, eucalyptol [10] Aqueous extract of Lavandula officinalis L., which contains phenolics and flavonoids such as caffeic acid, ferulic acid, gallic acid, rosmarinic acid, chlorogenic acid, umbelliferone, uteolin 7-O-glucoside, vitexin, and isoquercitroside [11] is suitable for phyto-nano synthesis. However, since lavender oil is used in the cosmetics and pharmaceutical industries, Lavender extract is a waste with a high potential for nanomaterial mass production by phyto-nano synthesis. Although most studies of phyto-nano synthesis are related to AgNP production, Horta-Piñeres et al. [12] reported that the method can also be applied in AgNW production. Phyto-nano synthesis can reduce metals to typically 4-100 nm in size[13]. The utilization of therapeutic herbs containing flavonoid and aromatic components stands out in studies [14]. Metal reduction and stability are performed with the help of secondary metabolites contained in plant extracts such as phenolic, terpenoids, alkaloids, and sugars [15]. Since plant extracts contain reducing agents, their effectiveness in nanoparticle synthesis is not surprising. However, it is quite surprising that a continuous nanoparticle such as AgNW can be produced simply in a non-polymerized aqueous medium.

While producing nano-silver materials with phyto-nano synthesis, the important factors that are not taken into account enough are light radiation and centrifuge effect. Although there are positive results in AgNP synthesis such as accelerating the synthesis of light and decreasing the particle size [16] we have seen that this is not the case when it comes to AgNW synthesis in our study with the phyto-nano synthesis method. In our study, we approached from a different angle and tried to define the negative effect of light radiation arising from its relationship with phenolics and an important positive effect provided by centrifuge.

2. Material and Method

2.1. Materials

2.1.1. Preparation of Lavandula officinalis L. flower extract

Lavandula officinalis L., Isparta / Turkey is local annual production. Harvested and natural dried lavender flowers were removed from their stems. The ratio of lavender extract prepared with deionized water is 1/100 (g/ml). Deionized boiled water was taken from the stove then plant samples were added and rested at room temperature for 1 hour. The mixture was filtered using a 0.2 µm Whatman® cellulose acetate membrane (19 °C and pH 5.7). All experiments have been at room temperature of 19-25 °C.

2.1.2. Phyto-nano synthesis of AgNPs and AgNWs

The $AgNO_3$ solution was prepared with 117 mg $AgNO_3$ (MERCK - 7761-88-8) and 100 ml deionized water. Lavandula extract and $AgNO_3$ solution were in a ratio of 1:1. Two experimental groups, one day and one week reaction time, were established to determine the centrifuge's rotation speed and time, as well as the effect of daylight and dark on the AgNW elongation that will occur with reduced AgNP. Hettich EBA 20 model centrifuge device, which we use to keep the rotation and gravity created by the centrifuge at maximum, was operated at 6000 rpm, which is the highest speed (in 37 sec.). Samples were filled into 10 ml tubes and centrifuged. Then deionized water was added to the pellet for washing, shaken gently and all samples were centrifuged again. This process was repeated at least twice according to the groups. Table of centrifuge amounts including washing process is given below (Table 1).

Table 1. Centrifuge time and repetitions at 6000 rpm according to light and dark application.

Reaction time	Centrifuge (min x repetitions)	
	Dark	*Light*
1 day (24h)	20X8	20X8
	5 X 3	5X3
1 week	20X8	20X8
	5 X3	5X3

2.2. Methods

2.2.1. Optical characterization of Ag nano particles

Surface plasmon resonance analysis applied for the optical characterization of metal nanoparticles provides guidance [17]. Perkin Elmer Lambda 35 UV-Vis Spectrophotometer device and crystal quartz tubs were used. In all of the measurements, the reaction time in the Mixtures was determined as 24 hours. Absorbances were scanned in the 200-800 nm light range in the samples.

Sample preparation for Scanning Electron Microscopy (SEM) and Energy Dispersive Spectrum (EDS)

To be used in the characterization analysis of silver nanoparticles SEM and EDS (Quanta Fec 250; The Thermo Scientific ™ Quanta ™), the sediments at the bottom of the tube were left to dry in a 50 °C oven after centrifuge. The residue adhering to the centrifuge tube was gently scraped and adhered to the carbon tapes.

Sample preparation for FTIR (Fourier transform infrared spectroscopy) and X-Ray Crystallography (XRD)

After the reactions in the dark and light, the extracts were poured into a glass petri dish and left to dry in a sterile oven at 50 °C for 48 hours to determine the organic content of the extracts. The resulting residues were scanned with the KBr pellet technique with 4000-400 cm^{-1} permeability. FTIR spectra (Perkin Elmer FTIR Spectrum BX) Infrared Spectroscopy Absorption Table (2020) was taken as a reference.
X-ray crystallography (XRD) analysis (Bruker D8 Advance Twin-Twin) of AgNW and AgNP samples in powder form synthesized in the dark was performed to determine the molecular composition and crystal structures of the silver nanoparticles.

Transmission Electron Microscope (TEM) analysis

Samples were dispersed with 1 ml of distilled water after centrifugation and stored in a light-proof bottle at room temperature. Hitachi HT7800 device was used for TEM analysis. The samples were dropped onto the carbon grid and dried at room temperature.

2.2.2. Biochemical analysis - HPLC (High-Performance Liquid Chromatography)

After 1 day of reactions, the supernatant after centrifuge of the mixture was taken to determine the relationship of light radiation to phenolics. HPLC determination of certain phenolics that are effective during AgNP production with lavender extract was made. These are generally composed of phenolics that have proven antioxidant properties. HPLC-wavelength was measured in DAD detector (λmax = 278nm). Mobile phase: consists of 3% acetic acid-methanol. Column sizes are 250x4.60 mm. and the particle diameter is 5 microns (Agilent Eclipse XDB-C18). Flow rate, 0.8 mL / min, column temperature, 300C; injection volume is 20 µl. (Agilent Eclipse XDB-C18). Flow rate, 0.8 mL / min, column temperature, 300C; injection volume is 20 µl.

3. Results

3.1. Production and morphological characterization of AgNP and AgNW by phytosynthesis

The first indicator in the silver reduction by phyto-synthesis is the color change in extracts [18]. When silver ions are reduced to Ag^0, the particle size in their aqueous solutions decrease and form clusters. In this way, the particle size of the resulting colloidal mixture becomes smaller than the visible light wavelength. Thus, the refracted light changes the color of the mixtures [19]. As can be seen in Figure 1, the color changes in reactions under dark and light differed from each other. Accordingly, it showed a brown-black color change in which AgNP reacted in light conditions (Figures 1A and 1B). In the dark, it showed a green-gray color change (Figure 1C).

Reduction of silver by phyto-nano synthesis has been demonstrated by brown color change [20]. It has been reported that aqueous solutions of silver nanowires are green-gray in color [21] This showed that the reaction took place by different mediators or produced different occurrences. The differences in extracts were analyzed to understand what caused this.

In the EDS analysis of the sample that was not washed, the spectra of Ag and the inorganic substances of the extract are shown (Figure 1A). After centrifugation, residues from lavender extract were removed (Figure 1B and C). With the effect of the centrifuge, AgNPs in the light reaction may show shape deformation and transform into plates (Figure 1B).). On the contrary, AgNPs preserved their stabilization in dark reactions and AgNW-like structures were formed (Figure 1C). Therefore, the light harmed particle stabilization and nanowire elongation. Plating occurred in all the irradiated samples, excluding the short light and centrifuged

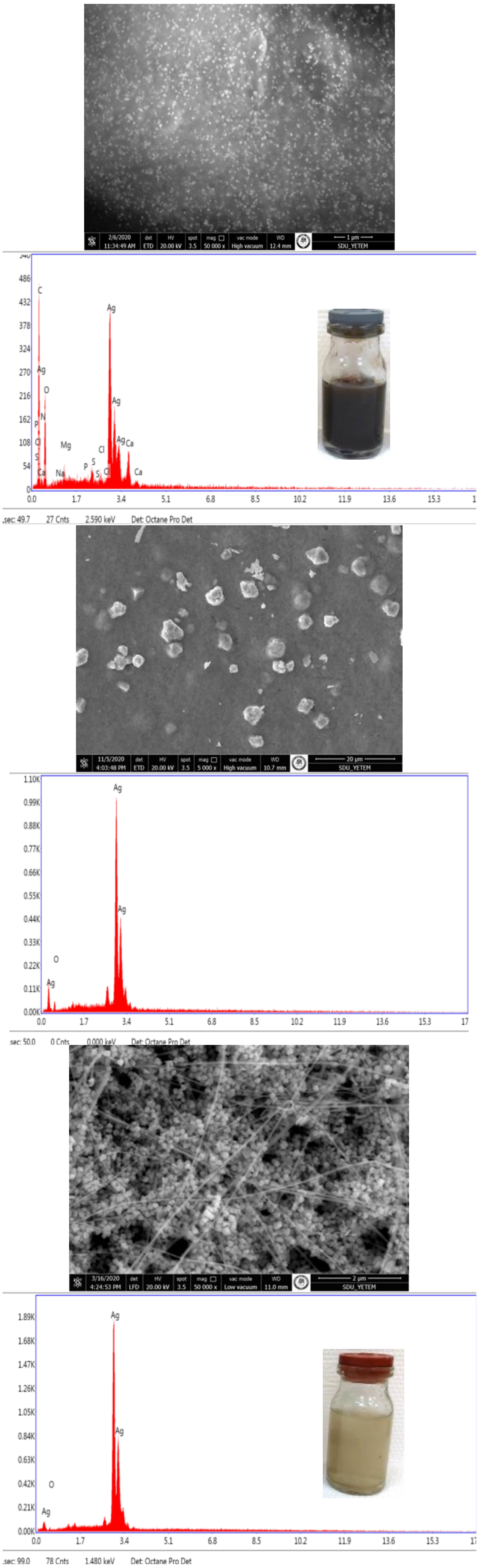

Figure 1. SEM and EDS analysis A: AgNPs in light environment B: AgNP under light and centrifuge effect C: AgNW in dark and centrifugal effect.

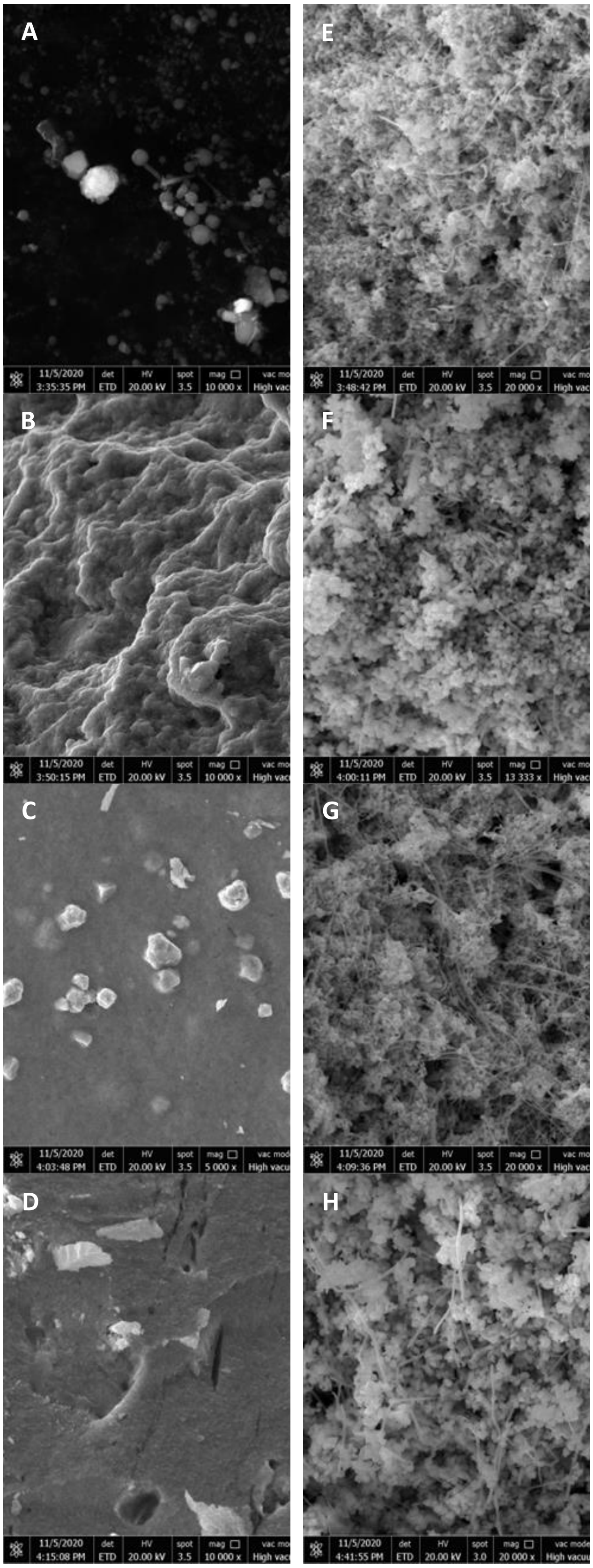

Figure 2. SEM images; on the left pictures the samples exposed to light A: 1 daylight 8 repetitions centrifuge B: 1 week light 8 repetitions centrifuge C: 1 daylight 3 repetitions centrifuge D: 1 week light 3 repetitions centrifuge. On the right pictures are dark-treated samples E: 1 day dark 8 repeat centrifuge F: 1 week dark 8 repeat centrifuge G: 1 day dark 3 repeat centrifuge H: 1 week dark 3 repeat centrifugation.

sample. Although nano rod-like structures were formed in this, no nanowire elongation occurred (Figure 2A). In all reactions in the dark application, it was determined that the particles preserved their shape stabilization well. Best AgNW elongation; It was obtained by reaction for 24 hours and centrifugation for a total of 15 minutes (Figure 2G).

The UV and Visible spectrum of AgNP surface resonances dispersed in an aqueous solution is around 400 nm [22]. In our study when the surface resonances of the reaction under light were scanned with UV-Vis, we obtained a peak that started at 311 nm and increased to 410 nm (Figure 3A). It was observed that the AgNP-specific 400 nm peak was weak in samples synthesized in the dark and not centrifuged (Figure 3B). On the other hand, in samples synthesized in the dark and not centrifuged, AgNP peaking at around 400 nm, AgNW at 377 nm and shows a rising value in the visible light region due to mixed nanoscale particles coincided with the literature [23,24]. In this case, it can be said that the silver reduced in the dark comes together with centrifugation to form AgNW.

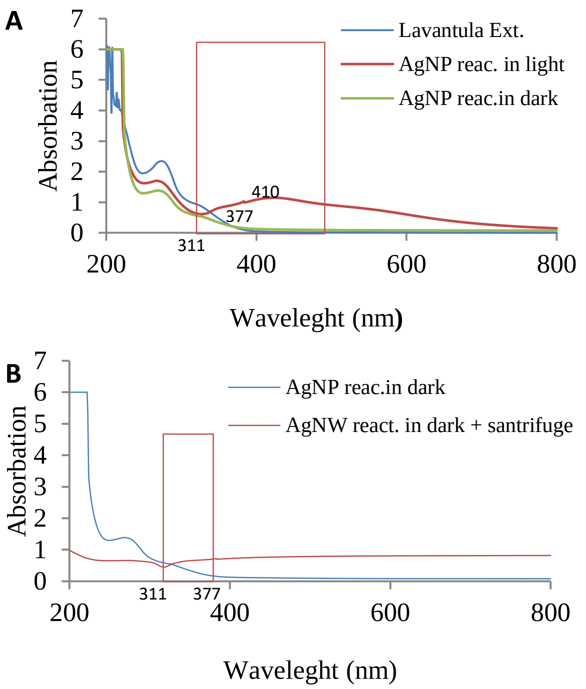

Figure 3. UV-Vis surface resonance spectra of particles in aqueous solution. A: Blue; Only lavender extract, Red at 24 hours light exposure; Lavender extract and $AgNO_3$ solution at 24 hours light exposure. Green; Lavender extract and $AgNO_3$ solution kept in the dark for 24 hours. B: Synthesis in the dark. Blue: not centrifuged. Red: centrifuged for a total of 15 minutes.

3.2. Structural characterization of AgNW

The most important feature of AgNW that makes it different from silver nanorods is that its aspect ratio is greater than 10^{-1}. Generally, AgNW has a 10-200 nm diameter and a length of 5-100 µm [9]. According to TEM images, AgNP sizes vary between 20 and 100

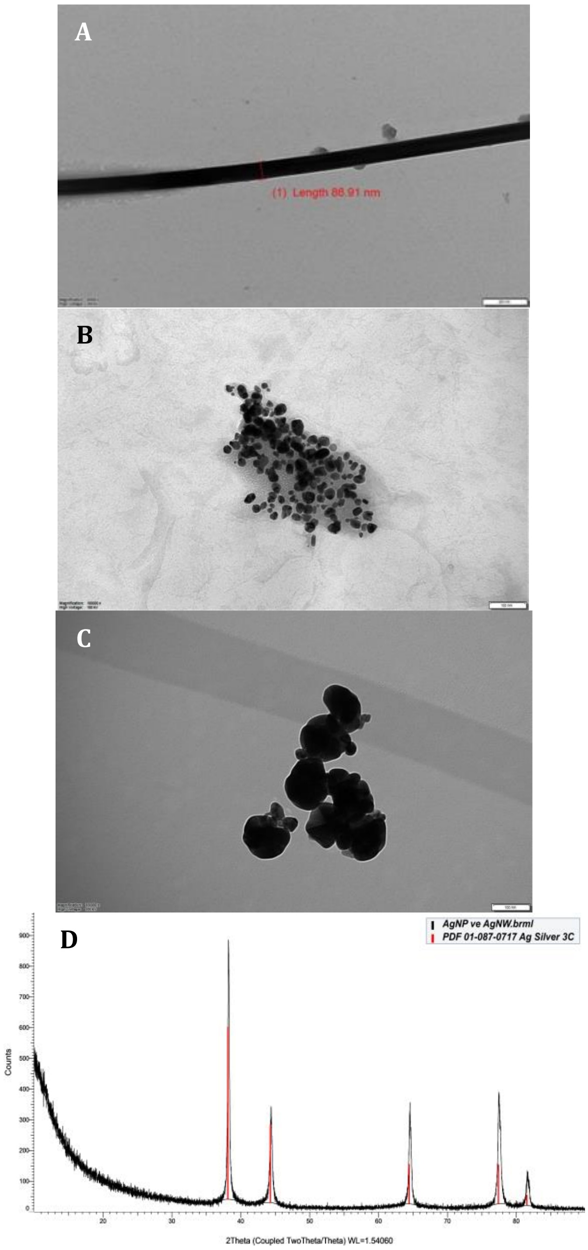

Figure 4. A: TEM image of AgNW synthesized in the dark with lavender extract B: Light exposure and sample not centrifuged C: non-centrifuged sample synthesized in the dark D: XRD pattern of Ag particles produced in dark.

nm. AgNW diameter varies between 40-100 nm and their length reaches 20 µm (Figure 4A). We did not find AgNW elongation in non-centrifuged samples (Figure 4B, C). According to XRD analysis performed to determine the crystal structure of powdered samples that are synthesized in the dark and containing AgNW, Ag particles have a face-centered cubic (Fcc) crystal structure (Figure 4D). According to the XRD patterns, the X-ray diffraction spectrum belonging to silver showed results complying with *Powder Diffraction* data (PDF) 01-087-0717. The values with a peak at 2θ (degree) indicate the planes (111), (200), (220), (311), (222), respectively, of the 38.119, 44.305, 64.452, 77.409, 81.552 Ag crystals. The ratio of (111) peak to (200) 2.21 and (220) to 4.34 when compared to the crystal model of standard silver powder (JCPDS; 2.1 and 4.0) compared to the density ratios obtained from the standard model of silver crystals with Fcc structure, the ratio of silver nanowires (200) shows that it may have a preferred orientation along the plane [25].

Light plays an effective role in reducing silver and decreasing particle size [26]. Although it shows different effects according to wavelengths and colors, light is a catalyst that allows the reduction reaction to take place in a shorter time [27]. Therefore, it is thought that daylight prevents the effect of the environment mechanics provided by the centrifuge in AgNW elongation and causes the time to pass during elongation to disappear. On the other hand, it can be predicted that silver bonds, which are effective in the elongation of silver atoms in a certain direction, cause an increase in the affinity of another atom in the extracted content, thus preventing the formation of Ag-Ag bonds.

3.3. The effect of artificial sunlight on phyto-synthesis reactions

To define the role of plant extracts in reducing the element silver and the effect of light, FTIR(Fourier transform infrared spectroscopy) analysis of only *Lavandula officinalis* leaf extract (LE) (Figure 5A), the extract containing $AgNO_3$ exposed to light (LS) (Figure 5B), and the extract containing $AgNO_3$ applied in the dark (DS) (Figure 5C) was performed.

The peaks between 3400 -3300 cm^{-1} are strong in Lavender extract (LE), medium in synthesis with light (B), and synthesis in dark (DS). These bands show the bonds (N-H) with the primary aliphatic amine group between the nitrogen of the nitrate group in $AgNO_3$ and aromatic phenolics. Bands saw at and around 2930 cm^{-1} indicate C-H vibrations of methyl, methylene, and aromatic hydrogens [28].

1715 cm^{-1} bands shown in all graphs of C=O vibrations belong to the ester, ketone, and carboxylic acid groups in the Lavender extract. The signals are seen at 1603 cm^{-1} in LE and 1612 cm^{-1} in LS and 1610 cm^{-1} in DS originate from C = C groups belonging to aromatic rings [29]. Taking stronger C=C vibrations in LE than LS and DS can be interpreted as the change of aromatic rings after the reaction. Bands seen at 1268 cm^{-1} in LE and 1262 cm^{-1} in LS may be due to C-O bonds originating from aromatic ester and alkyl aryl ether. As can be seen, a sharp band was not formed in this region in the reaction that took place in the dark (Figure 5C). It refers to the medium vibration imine/oxime-sourced C=N bonds seen at 1690-1640 cm^{-1} in LS and DS, but not in LE. These C=N bonds may have been formed from the bond formed between the C ends of the benzene rings that were broken after the reaction with the N of $AgNO_3$. This supports our notion that the synthesis of alkyl aryl ether similar to the Ullman reaction may have taken place. In this Ullman-like reaction, which may

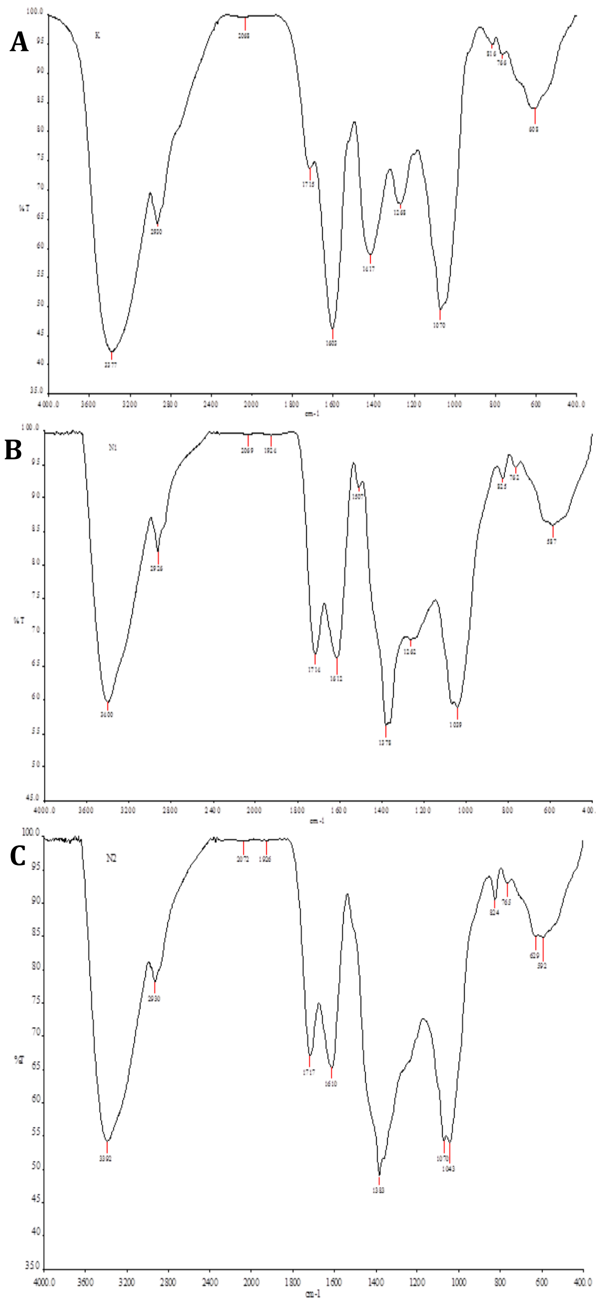

Figure 5. FT-IR spectra. A: Lavender extract B: extract after phyto-nano synthesis with 24 hours of light exposure. C: extract after phyto-nano synthesis applied in dark for 24 hours.

have occurred in the presence of phenolics and metals, the reduced Ag may have been the source of the metal. Light radiation may have replaced the required thermal source as a catalyst [30, 31, 32]. Therefore, the absence of a band around 1260 cm^{-1} in DS may prove that radiation-induced alkyl aryl reaction does not occur. Bands that are not observed in LE but shown at 1043 cm^{-1} in DS at 1039 cm^{-1} in LS and also around 1390 cm^{-1} (1378 cm^{-1} in LS and 1383 cm^{-1} in DS) show the presence of NO_3 from silver nitrate [33]. The sharp band at 1383 cm^{-1} in DS shows the presence of more free NO_3 than LS and that free Ag is more than LS, indicating that DS is more qualified in reducing silver. At 1070 cm^{-1}, when the C-O, C-O-C group bands are evaluated, they show sharper alcohol group vibrations in LE than LS and DS and sharper in DS than LS [34]. In other words, there are more alcohol groups in DS after the reactions than in LE. Considering the results, it is supported the thesis that light radiation acts as a catalyst on cyclic compounds containing the alcohol functional group in the presence of AgNP.

Compounds in plant extracts are responsible for the reduction of silver by phytosynthesis. The fact that the plants used are generally medical plants constitutes the opinion that the main effective mechanism is the secondary metabolites of the plant. According to FTIR results, the most important difference in the dark and light reaction may be the cyclic compounds containing the alcohol group, showing that phenolics, which are an important compound in the plant extract in reduction should be further investigated. After the syntheses made in light and dark were precipitated by centrifugation, 23 flavonoids that were mostly found in the herbal extract were scanned in the HPLC analysis we carried out on the plant extracts (Figure 6A).

The standard chromatogram includes *gallic acid*, *protocatechuic acid*, *catechin*, *p-hydroxybenzoic acid*, *chlorogenic acid*, *caffeic acid*, *epicatechin*, *syringic acid*, *vanillin*, *p-coumaric acid*, *ferulic acid*, *sinapinic acid*, *benzoic acid*, *o-coumeric acid*, *ferulic acid*, *hesperidin*, *rosmarinic acid*, *eriodictiol*, *cinnamic acid*, *quercetin*, *luteolin*, *kaempferol*, *apigenin* (Figure 6). Since the contents of *gallic acid*, *p-hydroxybenzoic acid*, *caffeic acid*, *epicatechin*, *syringic acid*, and *p-coumaric acid* differ significantly, quantification was made (Table 2). This difference in the quantity of flavonoids in the dark and light experiments suggests that light radiation in the presence of silver promotes photocatalysis that affects these flavonoids.

All components showed a decrease in both groups compared to the control except Epicatechin. The detection of Epicatechin in the light reaction in an even greater amount than in the control indicates that Epicatechin was synthesized under light catalysis during the reduction of silver. In the presence of light and silver, a polyflavone skeleton may be formed from aromatic ring compounds such as *syngric acid* and *p-coumeric acid* and *epicatechin* and its derivative molecule may be synthesized. Because, the positive effect of light on polyphenol synthesis is known [35]. This type of flavonoid synthesis was expressed through the synthesis pathways of *(-) epicatechin* and its *3-O-gallate* derivatives as Stadlbauer et al. [36] stated. According to the FTIR analysis of our study, the absence of vibrations of C-O bonds originating from aromatic esters and alkyl aryl ethers at 1268 cm^{-1} in LE and 1262 cm^{-1} in LS in DS supports our idea which is light catalysts in the reactions synthesized to *epicatehin* and its derivative polyphenols from other flavone skeletons (schematic theory Figure 7).

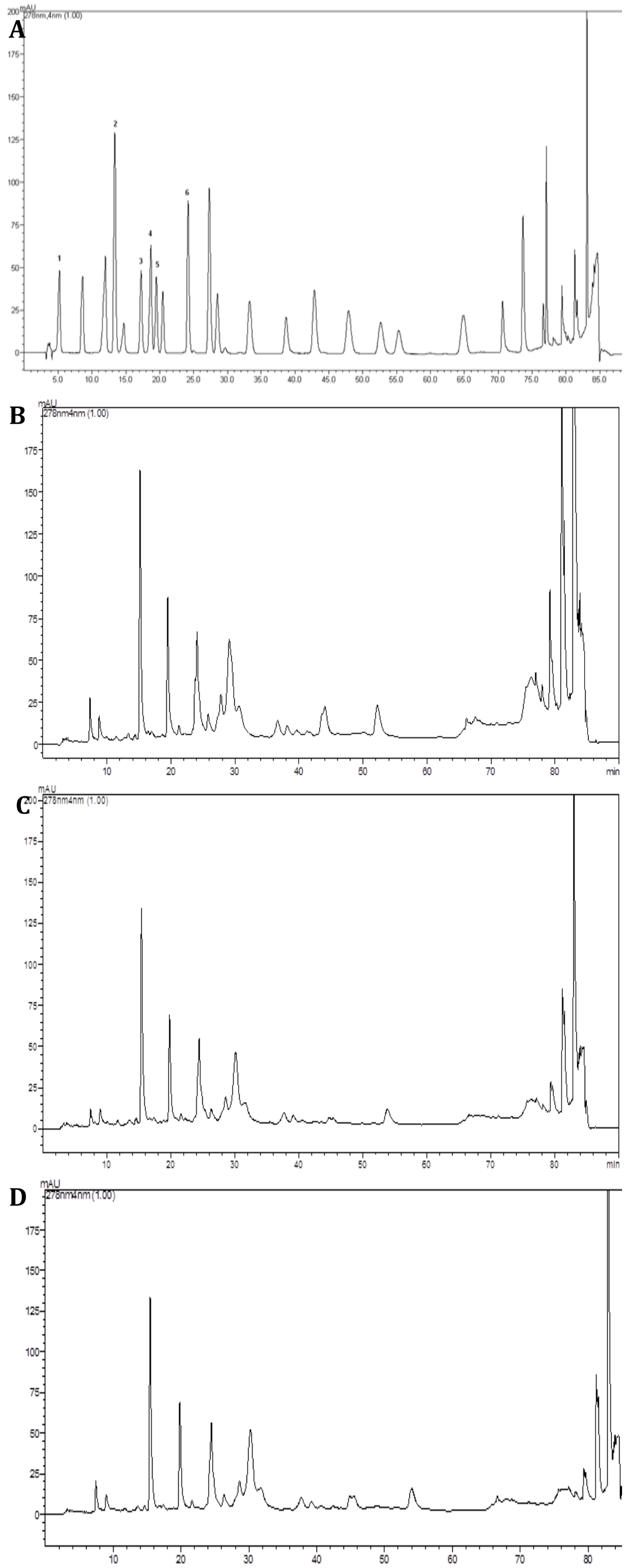

Figure 6. A: Standard chromatogram: 1: gallic acid 2: protocatechuic acid 3: catechin 4: p-hydroxybenzoic acid 5: chlorogenic acid 6: caffeic acid 7: epicatechin 8: syringic acid 9: vanillin 10: p-coumaric acid 11: ferulic acid 12: sinapinic acid 13: benzoic acid 14: o-coumeric acid 15: ferulic acid 16: hesperidin 17: rosmarinic acid 18: eriodictiol 19: cinamic acid 20: quercetin 21: luteolin 22: kaempferol 23: apigenin B: 1% (g / ml) lavender extract control C: Lavender extract irradiated for phyto-nano synthesis D: Dark lavender extract for phyto-nano synthesis

Table 2. Some flavonoid value of Lavender extracts used in phyto-synthesis *(ppm)*.

	Gallic acid	*p-Hydroxy benzoic acid*	*Caffeic acid*	*Epicatechin*	*Syringic acid*	*p-Coumaric acid*
Lavender extract (control)	0.2	0.9	2.2	3.6	14.5	5.3
Synthesis in dark	0.1	0.6	1.6	2.8	13.5	4.7
Synthesis with light	0.1	0.7	1.9	4.2	13.3	4.5

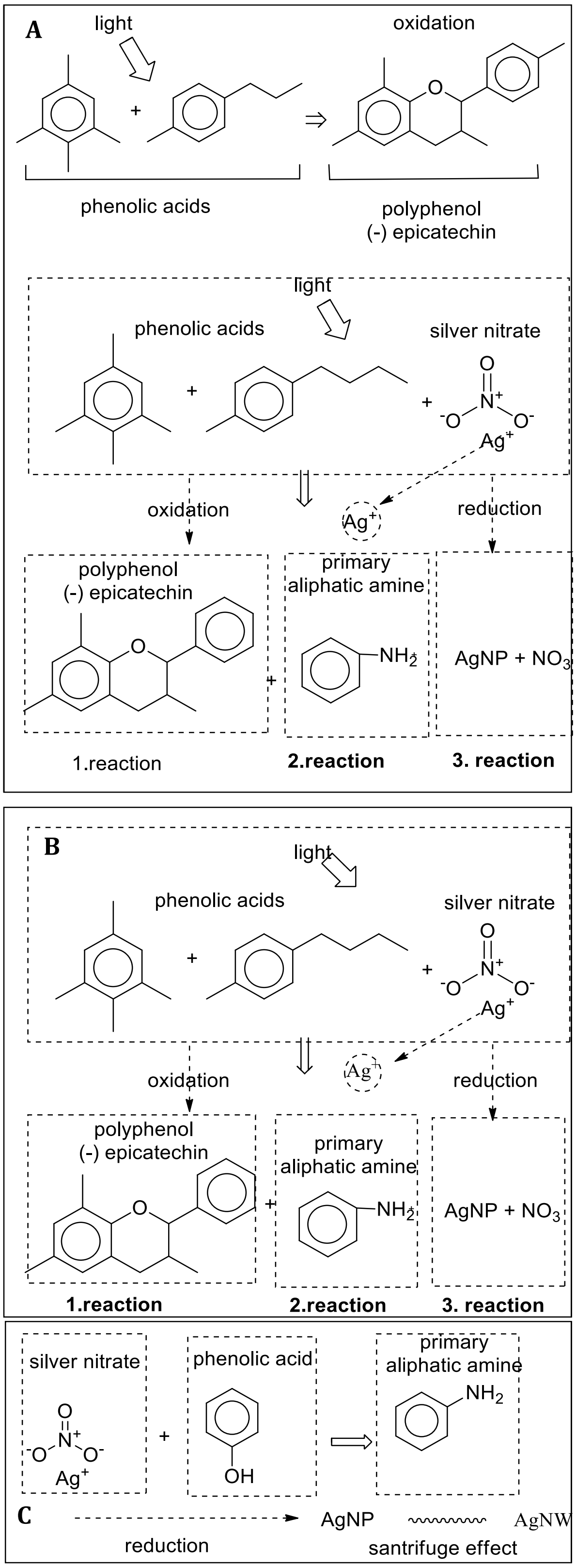

Figure 7. Schematic theory: A: possible epicatechin synthesis and Ag reduction and primer aliphatic amin sytesis with metal (Ag) nanoparticles in B: light C: dark.

4. Discussion and Conclusion

A photocatalysis occurred in the specified artificial daylight region, as supported by the color change in the lavender extract and another character analysis. Our study reveals the linear relationship of AgNW elongation by rotating the reduced silver particles counterclockwise in an aqueous medium and increasing gravity (centrifugation) in this direction. The reason why AgNW synthesis is almost absent in the light environment is probably that the reaction catalyzed by light accelerates AgNP synthesis but prevents AgNW synthesis [37]. In FTIR results, the stronger peaks of the bands belonging to the alcohol groups in dark application strengthen the idea that light-catalyzed reactions may be more effective in components containing alcohol. The difference in the number of flavonoids measured after light and dark reactions suggests that the cyclic compounds in the extract may be effective in photocatalysis. In another aspect, it may be using silver as the source in the reaction during photocatalysis and preventing the silver atoms from sticking together for AgNW elongation. In this method we propose, a polymer mold is not required to guide the shape of the particles, as in the soft-template method, to produce nanowires. On the contrary, the mechanics of the aqueous environment provided by centrifugation enable the elongation of the nanoparticles. The method is based on simple, ecological, and economical chemical and kinetic principles. It takes place with low energy consumption at low temperatures.

However, the synthesis of AgNW with this technique requires improvement even though it is a guide to cheap and easy production. Our work can act as a guide for chemical engineers in the design of processes so that the herbal extracts that are produced as waste in the cosmetics, pharmaceutical, and food industries in the future can be used in AgNW synthesis.

Declaration of Ethical Code

In this study, we undertake that all the rules required to be followed within the scope of the "Higher Education Institutions Scientific Research and Publication Ethics Directive" are complied with, and that none of the actions stated under the heading "Actions Against Scientific Research and Publication Ethics" are not carried out.

References

[1] Chandra, H., Kumari, P., Bontempi, E., Yadav, S. 2020. Medicinal plants: Treasure trove for green synthesis of metallic nanoparticles and their biomedical applications. Biocatalysis and Agricultural Biotechnology, 24, 101518.

[2] Salleh, A., Naomi, R., Utami, N. D., Mohammad, A. W., Mahmoudi, E., Mustafa, N., & Fauzi, M. B. 2020. The potential of silver nanoparticles for antiviral and antibacterial applications: A mechanism of action. Nanomaterials, 10(8), 1566.

[3] Jiang, H., Yan, X., Miao, J., You, M., Zhu, Y., Pan, J., Wang, L., Cheng, X. 2021. Super-conductive silver nanoparticles functioned three-dimensional CuxO foams as a high-pseudocapacitive electrode for flexible asymmetric supercapacitors. Journal of Materiomics, 7(1), 156-165.

[4] Kwon, J., Suh, Y. D., Lee, J., Lee, P., Han, S., Hong, S., Yeo, J., Lee. H., Ko, S. H. 2018. Recent progress in silver nanowire based flexible/wearable optoelectronics. Journal of Materials Chemistry C, 6 (28), 7445-7461.

[5] Liu, W. J., Liu, M. L., Lin, S., Liu, J. C., Lei, M., Wu, H., Dai, C. Q., Wei, Z. Y. 2019.Synthesis of high quality silver nanowires and their applications in ultrafast photonics. Optics Express, 27(12), 16440-16448

[6] Williams, N. X., Noyce, S., Cardenas, J. A., Catenacci, M., Wiley, B. J., Franklin, A. D. 2019. Silver nanowire inks for direct-write electronic tattoo applications. Nanoscale, 11(30), 14294-14302.

[7] Yu, Z., Li, L., Zhang, Q., Hu, W., Pei, Q. 2011. Silver nanowire-polymer composite electrodes for efficient polymer solar cells. Advanced Materials, 23(38), 4453-4457.

[8] Lah, N. A. C., Trigueros, S. 2019. Synthesis and modelling of the mechanical properties of Ag, Au and Cu nanowires. Science and Technology of Advanced Materials, 20(1), 225-261.

[9] Zhang, P., Wyman, I., Hu, J., Lin, S., Zhong, Z., Tu, Y., Huang, Z., Wei, Y. 2017. Silver nanowires: Synthesis technologies, growth mechanism and multifunctional applications. Materials Science and Engineering: B, 223, 1-23.

[10] Chen, L., Huo, Y., Han, Y. X., Li, J. F., Ali, H., Batjikh, I., Hurh, J., Pu, Y.J., Yang, D. C. 2020. Biosynthesis of gold and silver nanoparticles from Scutellaria baicalensis roots and in vitro applications. Applied Physics A, 126, 1-12.

[11] Radulescu, C., Stihi, C., Ilie, M., Lazurcă, D., Gruia, R., Olaru, O. T., Bute, O., C., Dulama, I., D., Stirbescu R. M., Teodorescu, S., Florescu, M. 2017. Characterization of Phenolics in *Lavandula angustifolia*. Analytical Letters, 50(17), 2839-2850.

[12] Horta-Piñeres, S., Hurtado, R. B., Avila-Padilla, D., Cortez-Valadez, M., Flores-López, N. S., Flores-Acosta, M. 2020. Silver nanoparticle-decorated silver nanowires: a nanocomposite via green synthesis. Applied Physics A, 126(1), 15.

[13] Borase, H.P., Salunke, B.K., Salunkhe, R.B., Pati, C.D., Hallsworth, J.E., Kim, B.S., Patil, S.V. 2014. Plant extract: a promising biomatrix for ecofriendly, controlled synthesis of silver nanoparticles. Applied Biochemistry and Biotechnology, 173(1), 1-29.

[14] Wang, Y., O'Connor, D., Shen, Z., Lo, I.M, Tsang, D.C., Pehkonene, S., Pu, S., Hou, D. 2019. Green synthesis of nanoparticles for the remediation of contaminated waters and soils: Constituents, synthesizing methods, and influencing factors. Journal of Cleaner Production, 226, 540-549.

[15] Rana, A., Yadav, K., Jagadevan, S.A., 2020. comprehensive review on green synthesis of nature-inspired metal nanoparticles: Mechanism, application and toxicity. Journal of Cleaner Production, 272, 122880.

[16] Wang, J., Zhang, S., Shi, Z., Jiu, J., Wu, C., Sugahara, T., Nagao, S., Suganuma, K., He, P. 2018.Nanoridge patterns on polymeric film by a photodegradation copying method for metallic nanowire networks. Royal Society of Chemistry Advances, 8(71), 40740-40747.

[17] Begum, R., Farooqi, Z. H., Naseem, K., Ali, F., Batool, M., Xiao, J., Irfan, A. 2018. Applications of UV/Vis spectroscopy in characterization and catalytic activity of noble metal nanoparticles fabricated in responsive polymer microgels: a review. Critical Reviews in Analytical Chemistry, 48(6), 503-516.

[18] Yousaf, H., Mehmood, A., Ahmad, K. S., Raffi, M. 2020. Green synthesis of silver nanoparticles and their applications as an alternative antibacterial and antioxidant agents. Materials Science and Engineering: C, 112, 110901.

[19] Vaidyanathan, R., Gopalram, S., Kalishwaralal, K., Deepak, V., Pandian, S. R. K., Gurunathan, S. 2010. Enhanced silver nanoparticle synthesis by optimization of nitrate reductase activity. Colloids and surfaces B: Biointerfaces, 75(1), 335-341.

[20] Fatima, R., Priya, M., Indurthi, L., Radhakrishnan, V., Sudhakaran, R. 2020. Biosynthesis of silver nanoparticles using red

algae Portieria hornemannii and its antibacterial activity against fish pathogens. Microbial Pathogenesis, 138, 103780.

[21] Cao, K., Yang, H., Gao, L., Han, Y., Feng, J., Yang, H., Zhang, H., Wang, W., Lu, Y. 2020 .In situ mechanical characterization of silver nanowire/graphene hybrids films for flexible electronics. International Journal of Smart and Nano Materials, 11(3), 265-276.

[22] Ezra, L., O'Dell, Z.J., Hui, J., Riley, K.R. 2020. Emerging investigator series: quantifying silver nanoparticle aggregation kinetics in real-time using particle impact voltammetry coupled with UV-vis spectroscopy. Environmental Science: Nano, 7(9), 2509-2521.

[23] Parente, M., Van Helvert, M., Hamans, R.F., Verbroekken, R., Sinha, R., Bieberle-Hütter, A., Baldi, A. 2020. Simple and Fast High-Yield Synthesis of Silver Nanowires. Nano Letters, 20(8), 5759-5764.

[24] Liu, L., He, C., Li, J., Guo, J., Yang, D., & Wei, J. 2013. Green synthesis of silver nanowires via ultraviolet irradiation catalyzed by phosphomolybdic acid and their antibacterial properties. New Journal of Chemistry, 37(7), 2179-2185.

[25] Kim, T. Y., Kim, W. J., Hong, S. H., Kim, J. E., Suh, K. S. 2009. Ionic-Liquid-Assisted Formation of Silver Nanowires. Angewandte Chemie International Edition, 48(21), 3806-3809.

[26] Lu, Z., Meng, M., Jiang, Y., Xie, J. 2014. UV-assisted in situ synthesis of silver nanoparticles on silk fibers for antibacterial applications. Colloids and Surfaces A: Physicochemical and Engineering Aspect, 447, 1-7.

[27] Srikar, S. K., Giri, D. D., Pal, D. B., Mishra, P. K., Upadhyay, S. N. 2016.Light induced green synthesis of silver nanoparticles using aqueous extract of Prunus amygdalus. Green and Sustainable Chemistry, 6(1), 26-33.

[28] Vlnieska, V., Zakharova, M., Börner, M., Bade, K., Mohr, J., Kunka, D. 2018. Chemical and Molecular Variations in Commercial Epoxide Photoresists for X-ray Lithography. Applied Sciences, 8(4), 528.

[29] Badri, K.B.H., Sien, W.C., Shahrom, M.S.B.R., Hao, L.C., Baderuliksan, N.Y., Rabbi'atul, N., Norzali, A. 2010. FTIR spectroscopy analysis of the prepolymerization of palm-based polyurethane. Journal of Solid State Science and Technology, 18 (2), 1-8.

[30] Javaherian, M., Kazemi, F., Ayati, S.E., Davarpanah, J., Ramdar, M. 2017. A tandem scalable microwave-assisted Williamson alkyl aryl ether synthesis under mild conditions. Organic Chemistry Research, 3(1), 73-85.

[31] Clavé, G., Garel, C., Poullain, C., Renard, B.L, Olszewski, T.K., Lange, B., Shutcha, M., Faucon, M.P., Grison, C. 2016. Ullmann reaction through ecocatalysis: insights from bioresource and synthetic potential. Royal Society of Chemistry Advances, 6(64), 59550-59564.

[32] Gutzler, R., Cardenas, L., Lipton-Duffin, J., El Garah, M., Dinca, L. E., Szakacs, C. E., ... & Rosei, F., Fu, C., Gallagher, M., Vondráček, M., Rybachuk, M., Perepichka, D.F. 2014. Ullmann-type coupling of brominated tetrathienoanthracene on copper and silver. Nanoscale, 6(5), 2660-2668.

[33] El-Kabbany, E., Badr, Y., Tosson, M., Taha, S., Mahrous., S. A. 1986. Detailed IR Study of the Order-Disorder Phase Transition of $AgNO_3$. Physica Status Solidi (a), 94(1), 35-43.

[34] Chen, X., Zhang, L., Qian, C., Du, Z., Xu, P., Xiang, Z. 2020. Chemical compositions of essential oil extracted from Lavandula angustifolia and its prevention of TPA-induced inflammation, Microchemical Journal. 153, 104458.

[35] Lu, Z., Liu, Y., Zhao, L., Jiang, X., Li, M., Wang, Y., Xu, Y., Gao, L., Xia, T. 2014. Effect of low-intensity white light mediated de-etiolation on the biosynthesis of polyphenols in tea seedlings. Plant Physiology and Biochemistry, 80, 328-336.

[36] Stadlbauer, S., Ohmori, K., Hattori, F., Suzuki, K. 2012. A new synthetic strategy for catechin-class polyphenols: concise synthesis of (−)-epicatechin and its 3-O-gallate. Chemical Communications, 48(67), 8425-8427.

[37] Bhaduri, G.A., Little, R., Khomane, R.B., Lokhande, S.U., Kulkarni., B.D., Mendis, B. G., Šiller, L 2013. Green synthesis of silver nanoparticles using sunlight. Journal of Photochemistry and Photobiology A: Chemistry, 258, 1-9.